

RESEARCH

Open Access



Multi-modal radiomics features to predict overall survival of locally advanced esophageal cancer after definitive chemoradiotherapy

Nuo Yu^{1†}, Yidong Wan^{2†}, Lijing Zuo^{1†}, Ying Cao^{1†}, Dong Qu³, Wenyang Liu¹, Lei Deng¹, Tao Zhang¹, Wenqing Wang¹, Jianyang Wang¹, Jima Lv¹, Zefen Xiao¹, Qinfu Feng¹, Zongmei Zhou¹, Nan Bi¹, Tianye Niu^{4*} and Xin Wang^{1*}

Abstract

Purpose To establish prediction models to predict 2-year overall survival (OS) and stratify patients with different risks based on radiomics features extracted from magnetic resonance imaging (MRI) and computed tomography (CT) before definite chemoradiotherapy (dCRT) in locally advanced esophageal squamous cell carcinoma (ESCC).

Methods Patients with locally advanced ESCC were recruited. We extracted 547 radiomics features from MRI and CT images. The least absolute shrinkage and selection operator (LASSO) for COX algorithm was used to obtain features highly correlated with survival outcomes in the training cohort. Based on MRI, CT, and the hybrid image data, three prediction models were built. The predictive performance of the radiomics models was evaluated in the training cohort and verified in the validation cohort using AUC values.

Results A total of 192 patients were included and randomized into the training and validation cohorts. In predicting 2-year OS, the AUCs of the CT-based model were 0.733 and 0.654 for the training and validation sets. The MRI radiomics-based model was observed with similar AUCs of 0.750 and 0.686 in the training and validation sets. The AUC values of hybrid model combining MRI and CT radiomics features in predicting 2-year OS were 0.792 and 0.715 in the training and validation cohorts. It showed significant differences in 2-year OS in the high-risk and low-risk groups divided by the best cutoff value in the hybrid radiomics-based model.

Conclusions The hybrid radiomics-based model demonstrated the best performance of predicting 2-year OS and can differentiate the high-risk and low-risk patients.

Keywords Esophageal squamous cell carcinoma, MRI, CT, Radiomics features, Prediction, Prognosis

[†]Nuo Yu, Yidong Wan, Lijing Zuo and Ying Cao contributed equally to this work.

*Correspondence:

Tianye Niu

niuty@szbl.ac.cn

Xin Wang

beryl_wx2000@163.com

Full list of author information is available at the end of the article



Introduction

Esophageal cancer (EC) is the seventh most common malignancy and ranks as the sixth leading cause of cancer mortality worldwide [1]. Despite the reductions in incidence rates attributed to economic growth and improved dietary structure, China still bears the highest burden of EC, particularly esophageal squamous cell carcinoma (ESCC). According to NCCN guidelines, definitive chemoradiotherapy (dCRT) is recommended for patients with unresectable or medically inoperable locally advanced ESCC. However, a multicenter study from China reported a 5-year overall survival (OS) of 30.0% following definitive radiotherapy for inoperable, locally advanced esophageal cancer and a 5-year OS of 22.0–27.7% for stage III to IV disease [2]. To further improve prognosis, effective predictors are needed to guide the individualized treatment.

In addition to clinical characteristics and biomarkers, imaging data are increasingly used to provide comprehensive information for clinical practice. Radiomics involves extracting high-throughput quantitative features from medical images and transforming these into mineable data to aid clinical decision-making [3, 4]. In EC, radiomics has advanced in clinical staging, prognosis prediction, treatment response evaluation and toxicity prediction [5–9]. However, research on prognosis prediction remains insufficient, and the unstable results require further validation. An increasing number of studies have highlighted that Magnetic Resonance Imaging (MRI) has significance in the diagnosis, staging and efficacy evaluation of EC [10–12]. Currently, the use of MRI-related radiomics in EC is in its early stages. Hirata et al. demonstrated that the histogram analysis of the Apparent Diffusion Coefficient (ADC) and basic parameters of Diffusion-weighted imaging (DWI) sequence in MRI could serve as biomarkers for pathological features and prognosis [13, 14]. A multi-modal radiomics model using MRI and CT was found to be more accurate in predicting tumor response after neoadjuvant chemotherapy in rectal cancer compared to MRI or CT alone [15]. However, no radiomics studies in ESCC have yet combined MRI and CT to establish models for prognosis prediction. Therefore, we hypothesised that the hybrid radiomics combining MRI and CT could improve the accuracy of the prediction models, enabling better differentiation between high- and low-risk patients.

This prospective study aimed to construct a multi-modal radiomics model combining MRI and CT scans to predict the 2-year OS and stratify patients with varying risks after dCRT in locally advanced ESCC.

Materials and methods

Patients

This study was approved by the Ethics Committee of Cancer Hospital of Chinese Academy of Sciences (ClinicalTrials.gov: NCT02988921) and conducted according to the Declaration of Helsinki. The clinical records and scan data of patients who met the inclusion criteria were collected from our database. Inclusion criteria: 1) ≥ 18 years old; 2) Clinical stages T1–4, N0–3, M0–1 (AJCC version 8, M1 stage is limited to lymph node metastasis in the supraclavicular area); 3) Radiation Equivalent Dose in 2 Gy/f (EQD2) ≥ 40 Gy was administered for primary site and lymph node metastases. 4) Minimum follow-up time was 2 years for surviving patients. Exclusion criteria: (1) The presence of previous malignancies (other than curable non-melanoma skin cancer or cervical cancer in situ) within 5 years; (2) An active infection requiring systemic treatment; (3) Pregnancy or lactation; (4) Patients with major cardiovascular and cerebrovascular arterial thromboembolism within 6 months prior to enrollment.

Primary treatment

All recruited patients received definitive chemoradiotherapy. According to our previous study, simultaneous integrated boost radiotherapy (SIB-RT) was performed with two dose levels: the planning gross tumor volume (PGTV) and planning target volume (PTV) were administered 59.92 Gy and 50.4 Gy, respectively, at 2.14 Gy and 1.8 Gy per fraction daily and 5 fractions per week [16]. The delineation of the target volume and the dose limits for organs at risk (OARs) were regulated by a multicenter phase III trial protocol [17]. Concurrent chemotherapy was based on a weekly regimen consisting of paclitaxel and platinum-based agents. This regimen included paclitaxel combined with either cisplatin or carboplatin.

Computed tomography (CT) and magnetic resonance (MR) image acquisition

The contrast-enhanced CT (CECT) images of the dataset were obtained from the CT simulator (Philips Brilliance CT Big Bore, Netherlands or Siemens SOMATOM Definition AS 40, Germany) before radiation therapy. The CT scan parameters were as follows: 120 kV; 180 effective mAs; beam collimation of 16×1.5 mm; a matrix of 512×512 ; a pitch of 0.813; and a gantry rotation time of 0.75 s. A dynamic contrast-enhanced CT scan was performed after intravenous administration of 2.0–2.5 ml/s nonionic contrast material (Ioversol Injection, 100 ml, 320 mg/ml, Hengrui, Jiangsu, China) using power injection at a rate of 3 ml/s followed by saline flush (20 ml). Arterial phase images were acquired at 43 s post-injection. The slice thickness of the reconstructed CT image was 5.0 mm. Arterial phase CT images were retrieved for image feature extraction.

Once the CT simulation was completed, the MRI images were performed using the MRI simulator (GE Discovery MR 750w 3.0T, General Electric Company, USA) to reduce the difference between CT and MRI images caused by body deformation. The MRI scan included high-resolution turbo T2-weighted imaging (T2WI), T2-weighted imaging fat suppression (T2WI-FS), and diffusion-weighted imaging (DWI). The radiomics features were extracted from the T2WI-FS sequence, and the parameters of this sequence were as follows: TR/TE=11250ms/78ms, frequency=352, FOV=480 mm×480 mm, bandwidth (KHz)=83.3, slice thickness(mm)=5, slice spacing(mm)=0.

Patients were included and randomized into the training and validation cohorts at a ratio of 7:3. Fig 1 shows the workflow of the study. After acquisition of the pre-treatment CT and MRI images, at least two radiotherapists with more than 10 years of experience each delineated the target volume, and another experienced radiotherapist reviewed the volume of interest (VOI).

The radiomic features were then extracted from the VOIs and screened. The features most associated with prognosis were selected to build the predictive models.

VOI acquisition and feature extraction

After patients underwent CT simulation scanning, the images were uploaded onto the Pinnacle system. Two radiologists with at least 10-year experience of imaging diagnosis and segmentation manually delineated the gross tumor volume (GTV), representing the primary tumor based on the CT images independently. Radiologists delineated the CT images while referencing corresponding MRI images to ensure accurate tumor boundary identification. Tumor areas were distinguished from normal tissues, such as the lungs, heart, and spinal cord, and gross tumor volumes were delineated as VOIs on CT images. These delineated VOIs on CT images were assumed to correspond with the VOIs on the MRI images after co-registration. Registration between CT and MR images was performed using the software (MIM

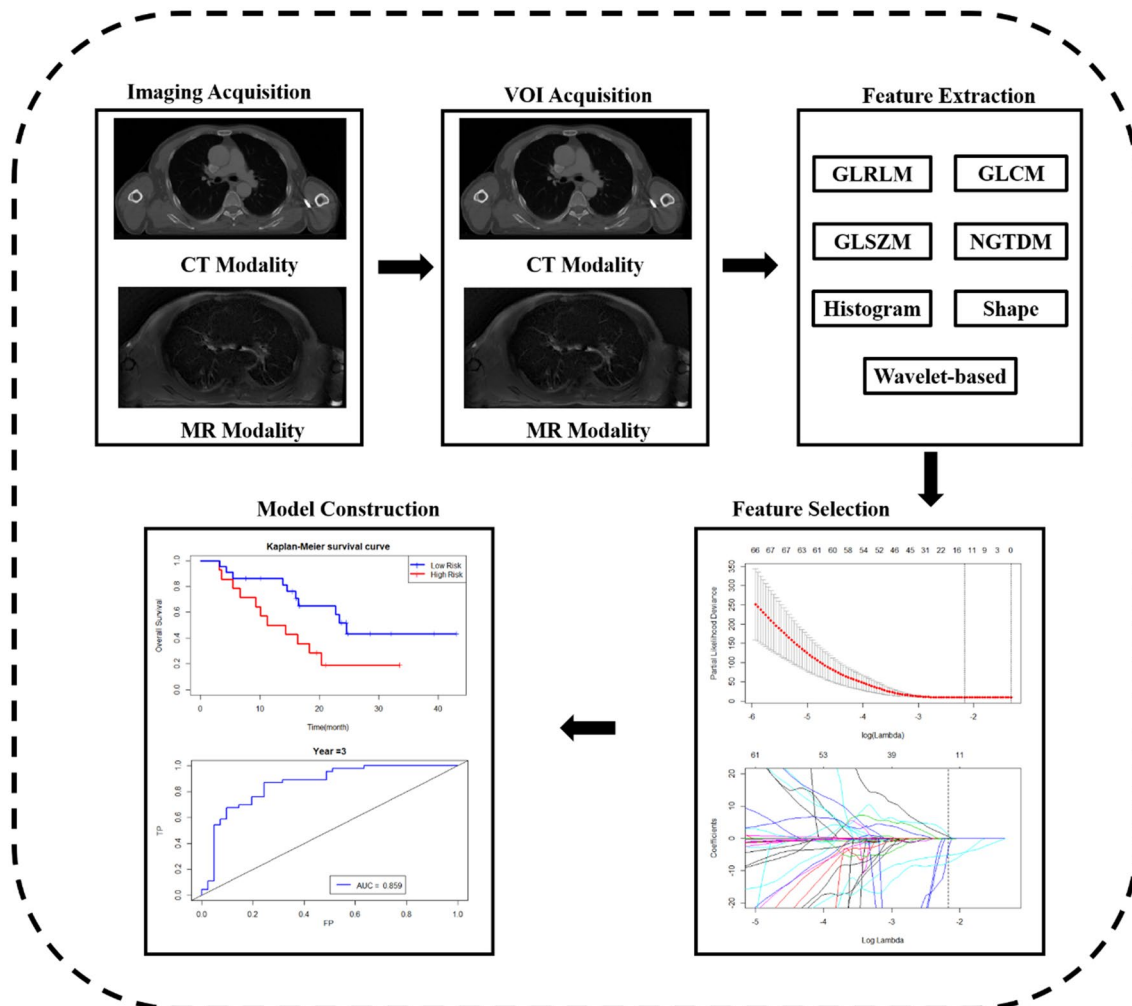


Fig. 1 The workflow of this study

SurePlan MRT, MIM Software Inc., Cleveland, USA). The VOIs from CT images were applied to MRI images following co-registration. Subsequently, to standardize image specifications across different CT and MR scanners, all slices were resampled to a $1 \times 1 \times 1 \text{ mm}^3$ voxel space size, and the grey levels were normalized to 64 levels for radiomics feature calculation [18]. For each modality, the MATLAB 2018b (MathWorks, Natick, MA, USA) software extracted 547 radiomics features [19]. These features include 7 shape features, 7 histogram features, 22 Gy-level co-occurrence matrix (GLCM) features, 13 Gy-level run-length matrix (GLRLM) features, 13 Gy-level size zone matrix (GLSZM) features, 5 neighborhood gray-tone difference matrix features (NGTDM), and 480 wavelet-based features [20]. A total of 1094 radiomics features including CT and MR modalities were extracted from each patient.

Radiomics feature selection and model construction

To eliminate the redundant features, an internal association assessment was conducted using the Pearson correlation method. The redundant features with high internal association (correlation coefficient (CC) > 0.90) were excluded [21]. Furthermore, the least absolute shrinkage and selection operator (LASSO) for Cox algorithm was used to identify features highly correlated with survival outcomes in the training cohort. The LASSO algorithm controls the number of selected variables by adjusting the parameter λ . The objective function of the LASSO algorithm is shown in Function (1), where y is the truth label, X is the feature matrix, β is the coefficients of features, and λ is the tuning parameter [22]. The LASSO method aims to minimize the objective function. As the value of λ increases, the coefficients of features decrease in magnitude. Only features with coefficients larger than zero are selected. The optimal λ in the LASSO algorithm was determined using 10-fold cross-validation. The λ resulting in the smallest mean difference between the predicted and actual survival in the cross-validations was used to select final factors. A radiomics score was derived from the selected features and their corresponding coefficients. The survival prediction model was constructed using the radiomics score and the Cox proportional hazards model.

$$\frac{1}{2} \|y - X\beta\|_2^2 + \lambda \|\beta\|_1 \quad (1)$$

Prognostic performance evaluation

The predictive performance of the radiomics score was evaluated in the training cohort and verified in the validation cohort using the concordance index (C-index). The patients were stratified into a low- or high-risk group based on the predicted risk using the proposed model.

The receiver operating characteristics (ROC) curves were used to determine the optimal cutoff risk for patient stratification. The Youden index was used to select the best cutoff value where the sum of sensitivity and specificity is maximized [23]. The Kaplan-Meier (KM) survival analysis and log-rank test were used to compare the difference between the survival curves of the two groups. The C-index and the area under the ROC (AUC) values for 2-year survival were used to compare the performance of the radiomics models based on MR, CT and hybrid modalities in the validation cohorts. Additionally, a clinical model was constructed for further comparison.

Statistical analysis

The endpoint of this study was the 2-year OS, which was defined as the time from the first day of radiotherapy to death or last follow-up. Statistical analysis was performed using R software (R Core Team. R: A language and environment for statistical computing. R Foundation for Statistical Computing, Vienna, Austria. URL: <http://www.R-project.org>, 2016). The Mann-Whitney U test and chi-q test were used to compare the difference in patient clinical characteristics in the two cohorts. Overall survival (OS) was calculated by the Kaplan-Meier method and compared using the log-rank test. Statistical significance was set at $P < 0.05$.

Results

Patient characteristics

The clinical characteristics of all patients are summarized in Table 1. 210 patients were recruited for this trial, and 18 patients were excluded, resulting in 192 patients being included (Fig. 2). A total of 132 patients received concurrent chemoradiotherapy, of whom 100 received paclitaxel and cisplatin and 32 received paclitaxel and carboplatin. Of the 192 patients, 135 were randomly assigned to the training cohort and 57 to the validation cohort in a 7:3 ratio. The median age of the two groups was 62 (range, 47–83 years) and 66 (range, 48–92 years), respectively. There was no difference between the training and validation groups in terms of gender, tumor location, tumor length, T stage, N stage, or total TNM stage, with or without concurrent chemotherapy and pre-treatment neutrophil to lymphocyte ratio (pre-NLR).

For the entire cohort, the median follow-up was 39.9 months. The median OS was 19.7 months (95% CI, 16.3 to 23.1 months), and the 2-year OS was 42.1%. The median OS in the training group was 19.5 months (95% CI, 15.5 to 23.4 months), and 19.8 months (95% CI, 11.9 to 27.8 months) in the validation group. The 2-year OS in training and validation groups was 41.5% and 43.7%, respectively.

Table 1 Baseline characteristics

Characteristics	Training cohort	Validation cohort	P-value
All	135 (70.3)	57 (29.7)	
Gender			0.083
Male	110 (81.5)	40 (70.2)	
Female	25 (18.5)	17 (29.8)	
Age (years)			0.002
Mean	62	66	
Range	47–83	48–92	
Tumor location			0.693
Cervical	3 (2.2)	3 (5.3)	
Upper	28 (20.7)	10 (17.5)	
Middle	71 (52.6)	28 (49.1)	
Lower	33 (24.4)	16 (28.1)	
Tumor length (cm³)			0.414
≤5	75 (55.6)	28 (49.1)	
>5	60 (44.4)	29 (50.9)	
T stage			0.335
T2	11 (8.1)	1 (1.8)	
T3	78 (57.8)	38 (66.7)	
T4a	39 (28.9)	16 (28.1)	
T4b	7 (5.2)	2 (3.5)	
N stage			0.576
N0	5 (3.7)	2 (3.5)	
N1	52 (38.5)	16 (28.1)	
N2	62 (45.9)	31 (54.4)	
N3	16 (11.9)	8 (14.0)	
M stage			0.015
M0	117 (86.7)	41 (71.9)	
M1	18 (13.3)	16 (28.1)	
cTNM stage			0.112
II	8 (5.9)	3 (5.3)	
III	62 (45.9)	22 (38.6)	
IVA	47 (34.8)	16 (28.1)	
IVB	18 (13.3)	16 (28.1)	
Concurrent Chemotherapy			0.122
Yes	89	44	
No	46	13	
Pre-NLR			0.194
Mean ± SD	2.67 ± 1.14	2.43 ± 1.15	
Range	0.89–7.42	0.95–6.14	

Abbreviation: Pre, pre-treatment; NLR, neutrophil to lymphocyte ration; SD, standard deviation

Feature selection and model evaluation

Firstly, 540 radiomics features were extracted from CT images. 241 features were retained after correlation analysis, and 8 features were used to construct a CT-based prediction model after LASSO feature selection through a ten-fold cross validation experiment (Fig S1). Secondly, 540 radiomics features were extracted from the MRI modality to construct a 2-year OS prediction model. We used the correlation analysis method to select 230

features. Then, the ten-fold LASSO algorithm selected 4 radiomics features to construct the MRI-based prediction model (Fig S2). In addition to single-modality analysis, we examined the performance of modality fusion. We fused two types of features for radiomics modeling. A total of 471 handcrafted features were retained after the correlation analysis process. Then, 6 features, including 2 CT-based features and 4 MRI-based features (CT_ZP_LHL, CT_Strength_HHH, MR_inf1h_LLL, MR_Busyness_LHL, MR_cprom_LHH, and MR_LZHGE_HHL) were retained through the LASSO algorithm (Fig S3). Considering the clinical predictive potential, we also ran the clinical model based on the clinicopathologic characteristics of the patients. A total of 21 clinical characteristics collected in this study (sex, age, tumor position, distance from the incisor to the upper boundary of the tumor, tumor length, clinical T, N, M and total stage, pre-treatment and nadir lymphocyte, neutrophil, neutrophil to lymphocyte ratio (NLR), hemoglobin, albumin and total protein) were selected using the LASSO method (Fig S4).

In the training cohort, the CT-based prediction model achieved a C-index score of 0.677 (95%CI: 0.562–0.791), and in the validation cohort, the prediction model produced a C-index score of 0.608 (95%:0.413–0.802). The C-index value of the MRI-based model was 0.685 (95%CI: 0.573–0.798) and 0.667 (95%CI: 0.484–0.851) for the training and validation cohorts, respectively. For the hybrid radiomics model, the training set achieved a C-index value of 0.716 (95% CI: 0.606–0.826), and the validation set achieved a C-index value of 0.667 (95% CI: 0.497–0.837). The proposed clinical model showed a lower prediction performance than all radiomics models, with a C-index of 0.656 (95%CI: 0.541–0.771) for the training cohort and 0.555 (95%CI: 0.340–0.769) for the validation cohort.

Subsequently, the AUC values for predicting 2-year OS were evaluated for two cohorts. The result showed an AUC of 0.733 for the training cohort and an AUC of 0.654 for the validation cohort in the CT-based model (Fig. 3A and B). The MRI-based model showed the AUCs of 0.750 and 0.686 for the training and validation cohorts, respectively (Fig. 3C and D). The hybrid model displayed the best performance among all models, with AUC values of 0.792 and 0.715 for the training and validation cohorts, respectively (Fig. 3E and F). The AUC values of the clinical model were lower than those of the radiomics-based models, with AUCs of 0.737 and 0.538 for the training and validation sets, respectively (Fig. 3G and H).

At the same time, we calculated a cutoff value based on Youden index with a radiomics score of 0.041, 0.013 and 0.005 in CT, MRI and hybrid radiomics models, respectively. The patients were divided into high-risk and low-risk groups based on the cutoff value. The KM

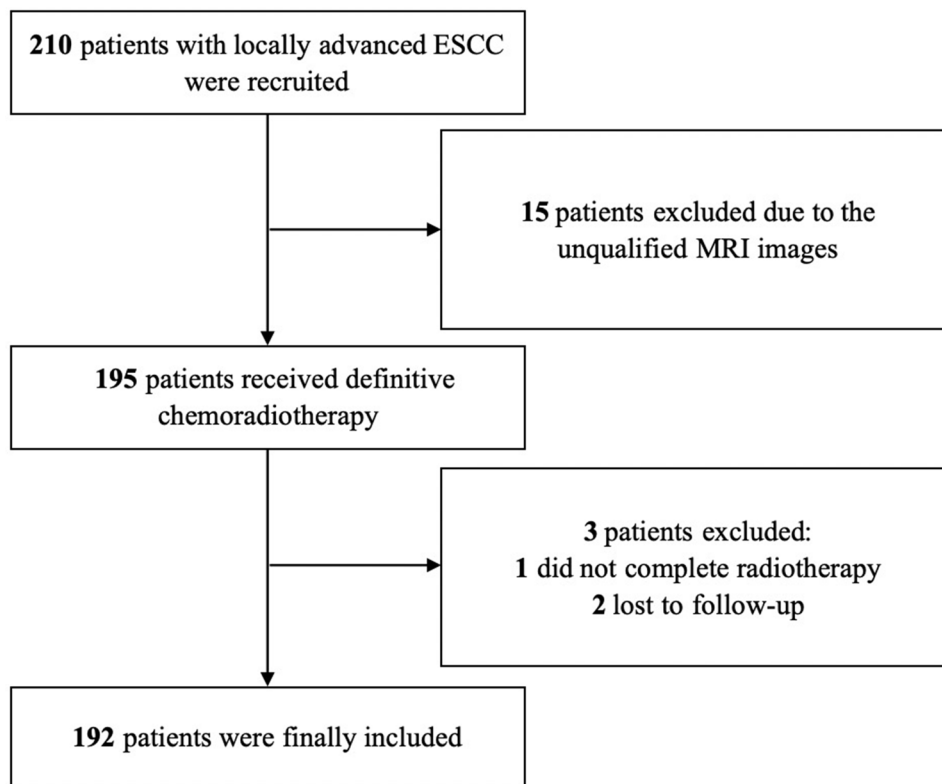


Fig. 2 CONSORT diagram

curves for OS showed a significant difference between the two groups of patients in the training and validation cohorts. The OS of the CT-based model for two groups are shown in Fig. 4A and B (low-risk and high-risk in the training group, $P < 0.001$: 2-year OS 67.2% vs. 27.1%; validation group: 2-year OS 62.0% vs. 30.3%, $P = 0.024$). For the MRI-based model, the p-value for OS between low-risk and high-risk patients was less than 0.05 in both the training and validation cohorts. The detailed OS curves are shown in Fig. 4C and D (low-risk and high-risk in training group: 2-year OS 71.2% vs. 22.9%, $P < 0.001$; validation group: 2-year OS 57.7% vs. 26.9%, $P = 0.012$). As for the hybrid model, a significant difference in OS was observed between low-risk and high-risk groups in both cohorts. The detailed OS KM curves involving two groups are also shown in the Fig. 4E and F (low-risk and high-risk in training group: 2-year OS 68.9% vs. 18.9%, $P < 0.001$; validation group: 2-year OS 55.3% vs. 23.8%, $P = 0.018$). The significant difference in OS between low-risk and high-risk patients was not observed in the clinical model with a p-value of 0.210. The OS was presented in Fig. 4G and H (low-risk and high-risk in training group: 2-year OS 59.7% vs. 20.6%, $P < 0.001$; validation group: 2-year OS 48.5% vs. 37.5%, $P = 0.210$).

Discussions

Our study constructed a multi-modal CT and MRI radiomics prediction model of CT and MRI features, which demonstrated potential to predict 2-year OS of ESCC patients. It showed that our radiomics model contributed more than the clinical model to the stratification of low-risk and high-risk patients in terms of overall survival. To our knowledge, this is the first study to predict the OS of ESCC patients using integrated CT and MRI radiomics features.

Compared to MRI-based radiomics, most results in EC radiomics come from positron emission tomography-computed tomography (PET-CT) and CT images [7, 24–27]. CT is the most basic imaging modality in the staging of EC. The CT images can be expediently obtained and reused to extract deeper information. Therefore, CT-based radiomics has made great progress in predicting the prognosis of patients with EC. A recent similar study led by Xie demonstrated the potential of CT radiomics and machine learning for diagnosing occult ESCC, highlighting radiomics' versatility across diagnostic and prognostic applications and conducted both internal and external validation, yielding reliable results [28]. Another study extracted sub-region based radiomics features from EC patients receiving (chemo)radiotherapy and confirmed that the sub-region based radiomics model had AUC values of 0.821 in the

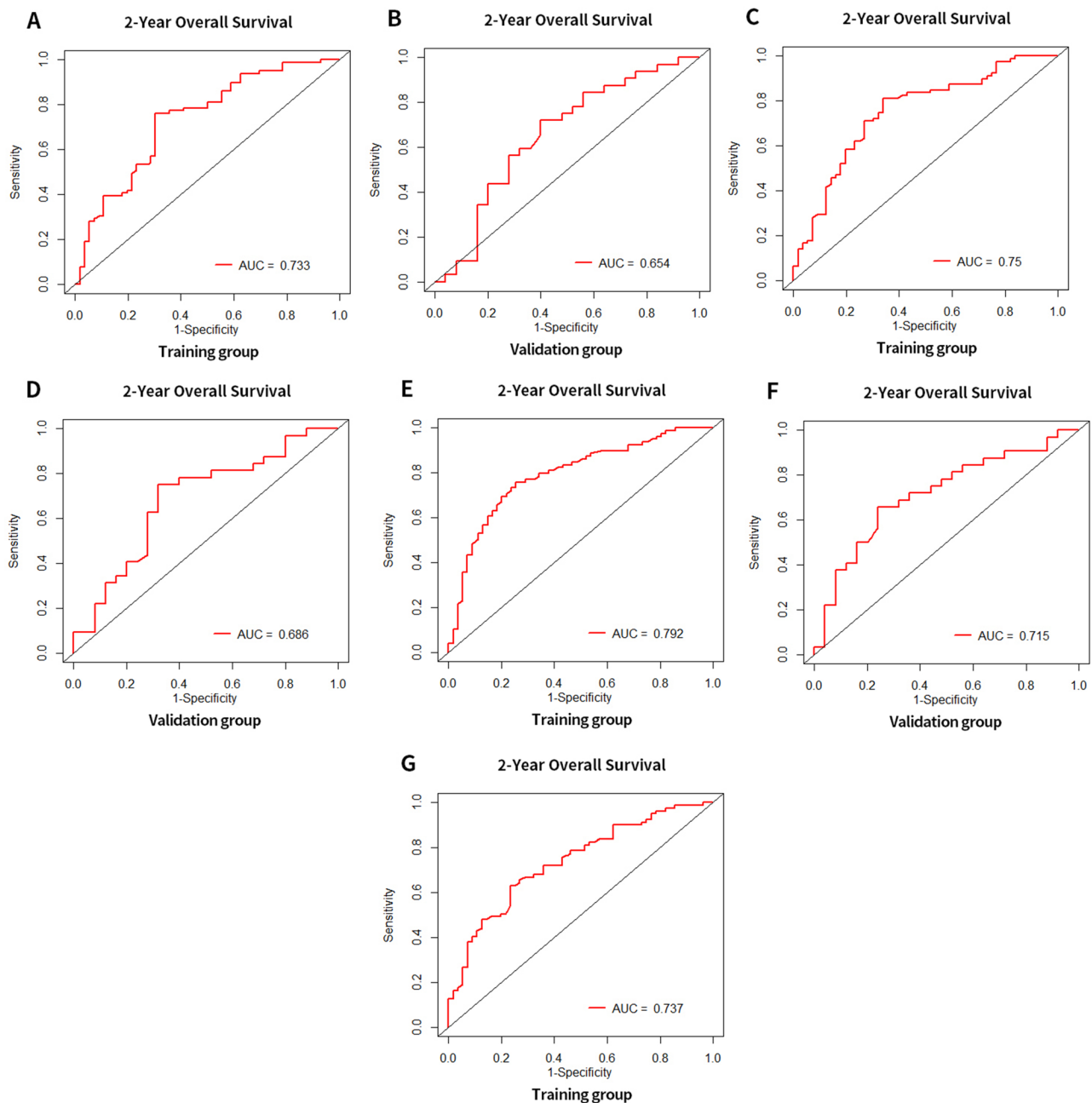


Fig. 3 The receiver operator characteristic (ROC) curves of the training cohort and validation cohort of CT based radiomics model (A, B), MRI based radiomics model (C, D), hybrid of CT and MRI based radiomics model (E, F) and clinical model (G, H)

training group and 0.805 in the validation group in predicting 2-year OS, higher than the AUC values of 0.733 and 0.654 in our study [22]. This may be due to the small number of patients in their experiment, only 87 in the training group and 46 in the validation group. Tang et al. further found that the combination of radiomics and clinical features performed better than either of them in predicting early recurrence of locally advanced ESCC (AUC values of combined group vs. radiomics group vs. clinical group in validation groups: 0.809 vs. 0.646 vs.

0.658) [26]. A multicenter study further developed and validated the hybrid radiomics nomogram of radiomics signatures, deep-learning signature and clinical factors in predicting local recurrence of ESCC patients after definitive (chemo)radiotherapy (C-index in training, internal validation and external validation set: 0.82 vs. 0.78 vs. 0.76) [29]. However, our study found that the predictive performance of clinical factors was lower than that of radiomics. Combining clinical factors with radiomics would reduce the accuracy of the prediction model.

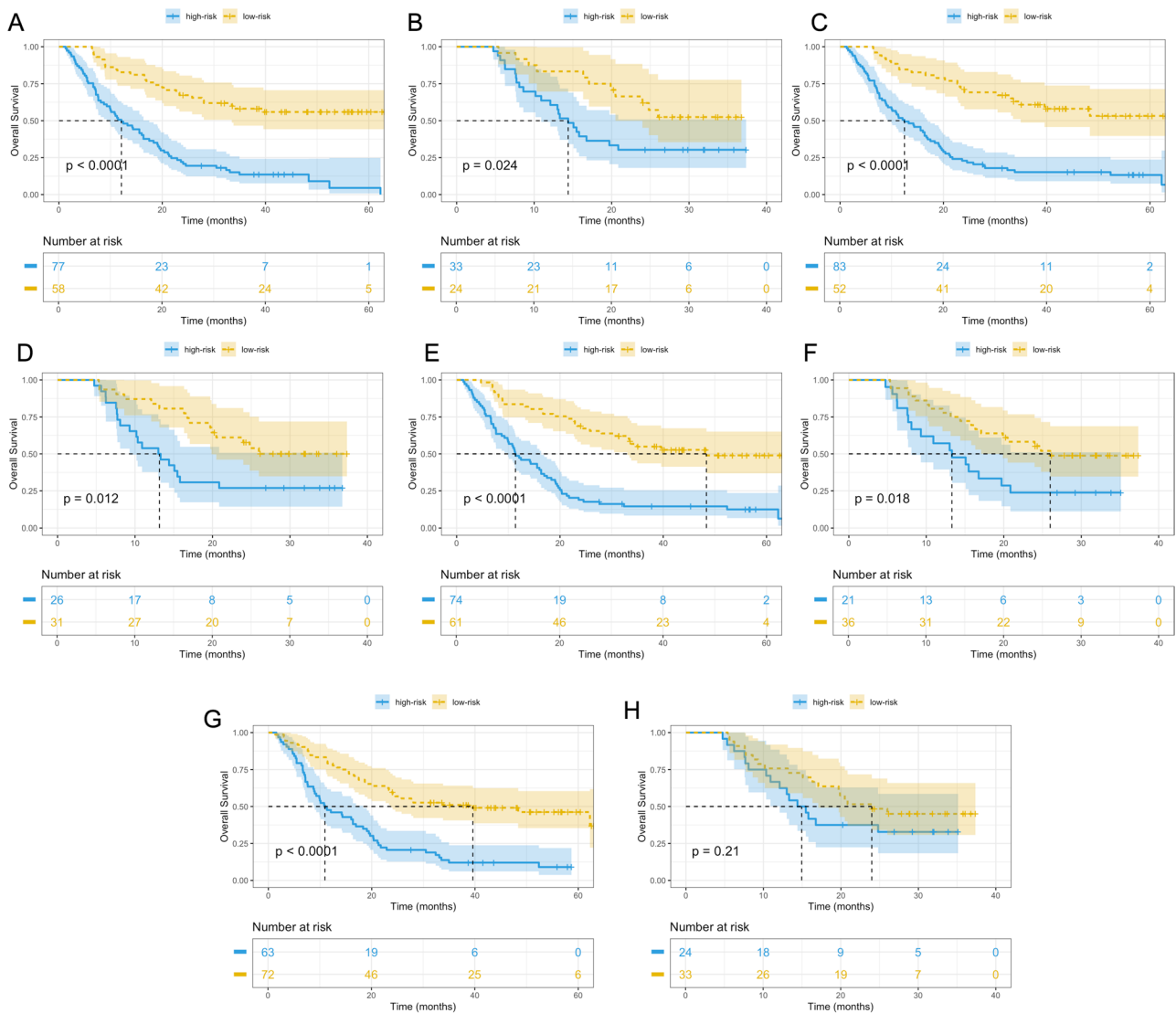


Fig. 4 The Kaplan-Meier curves of Overall Survival of training cohort and validation cohort of CT-based radiomics model (A, B), MRI-based radiomics model (C, D), the hybrid of MRI and CT based radiomics model (E, F) and the clinical model (G, H)

This may be due to the fact that the radiomics features had much better prediction performance than the clinical features, so adding clinical factors did not improve the accuracy of the model. Therefore, we did not include clinical factors in the integrated model.

Unlike the flourishing CT radiomics studies, MRI-based radiomics research is still relatively rare and in their infancy. Hirata et al. explored the relationship between apparent diffusion coefficient (ADC) related features and prognosis and demonstrated that histogram analysis of ADC could predict recurrence-free survival and disease-specific survival in ESCC patients [13]. Chu et al. constructed a combined model of MRI-based radiomics and clinical features and showed high accuracy in predicting OS (C-index in training and validation groups: 0.730 and 0.712) and DFS (C-index: 0.714 and

0.729) [30]. However, in our study, the clinical factors are less effective in predicting prognosis, but the combination of the two imaging radiomics has better predictive efficacy. MRI has been shown to be very useful in determining the T stage, particularly when the tumor is not clearly demarcated from the trachea and great vessels in EC [31, 32]. The combination of MRI and CT radiomics can provide additional information about tumor biological characteristics and heterogeneities, which are proved to be associated with the prognosis of patients with rectal cancer [33, 34]. Li et al. demonstrated that an MRI-based radiomics model was more effective than CT in predicting therapeutic response after neoadjuvant chemotherapy for locally advanced rectal cancer. The combination of MRI and CT radiomics achieved the highest AUC value of 0.925 in the training group and 0.93 in

the validation group [15]. However, no similar study on hybrid MRI and CT radiomics has been conducted in EC. MRI is rarely used in the diagnosis of EC due to respiratory movement and heartbeat affecting the sharpness of MRI imaging. Additionally, the coils used to scan the cervical and chest esophagus are different, making it possible to scan the entire esophagus once [35]. However, advancements in MRI technology have made long-range and whole-body MRI scans clinically available [36, 37]. Moreover, techniques such as the ultrasound-driven 4D MRI method and sensor systems have been developed for respiratory motion imaging and respiratory gating in thorax and abdomen scans [38, 39]. Additionally, MRI has certain advantages in staging T3 and T4 patients and determining resectability for surgeons in ESCC, making it an increasingly important tool in the diagnosis and treatment of EC.

This study found that the hybrid model had the best predictive ability compared to the MRI or CT models. Additionally, the MRI model performed slightly better than the CT model in predicting the 2-year OS of ESCC patients after dCRT, achieving an AUC of 0.715 in the validation group, which is better than some single-modal image studies [7, 27]. Moreover, the radiomics models were far more accurate than the clinical factors in terms of prediction accuracy. It is hypothesized that pre-treatment imaging captured more detailed and individual features of the patient group, thus better reflecting the tumor heterogeneity and providing the predictive value. Furthermore, the hybrid radiomics model was used to significantly stratify high-risk and low-risk patients, providing valuable guidance for the follow-up treatment of ESCC patients.

Recent studies have shown that combining radiomics with biomarkers such as HER2 and CD44 may lead to promising results in predicting prognosis [40]. Xie's study suggested a significant correlation between copy number alterations (CNA) and radiomics features [22]. The combination of genomics and radiomics may have greater predictive potential in clinical practice and may reveal biological pathways associated with cancer. In recent years, it has been confirmed that certain features in the image of pathological tissue can be used to predict survival in non-small cell lung cancer [41]. In rectal cancer, a combination of histopathological and radiomics features can predict tumor response better than three single-modality prediction models in terms of AUC values (0.812, 95%CI 0.717–0.907 vs. 0.630, 95%CI 0.507–0.754; 0.716, 95%CI 0.580–0.852; 0.733, 95%CI 0.620–0.845) [42]. In the future, the combination of multi-disciplinary omics may provide more prognostic information for survival prediction and model construction in ESCC. In addition, theranostics, integrating diagnostic imaging with therapy, exemplifies future imaging-based

treatment strategies. For instance, PET-CT radiomics combined with metabolic parameters has shown potential in assessing treatment responses and guiding personalized care for esophageal cancer [43–45]. Furthermore, artificial intelligence (AI)-driven radiomics models are advancing survival prediction and treatment stratification, enhancing diagnostic and therapeutic precision [46]. Future directions should focus on multi-omics integration and advanced machine learning techniques to enhance radiomics' clinical utility. These efforts may bridge diagnostic imaging with therapeutic applications, offering a comprehensive approach to esophageal cancer management.

Our study has some limitations. Firstly, it was a single-center clinical trial and lacked external validation. Secondly, the small patient cohort and limited imaging data may affect result accuracy. Another limitation of our study is the use of manual segmentation, which may be subject to variability. The segmentation method is crucial, as differences in manual segmentation among different physicians can be significant, leading to lower consistency. Future work could include a comparison of semi-automatic or automatic segmentation methods, as suggested by studies like Cairone et al., to improve accuracy and efficiency in tumor delineation and radiomics analysis [47]. Finally, to ensure high repeatability of images and positions, we acquired images of MRI positioning on the same day as CECT scans. As a result, contrast-enhanced MRI images were unavailable for analysis. Moreover, we did not include the ADC calculated from the DWI phase in our analysis. Further analysis of this data may enhance model prediction accuracy in the future.

In conclusion, multi-modal radiomics combining MRI and CT improved 2-year OS prediction in ESCC patients, outperforming single-modality radiomics and clinical features, and enabling better risk stratification.

Abbreviations

ADC	Apparent Diffusion Coefficient
ADC	Apparent diffusion coefficient
AUC	Area under the ROC
CT	Computed tomography
CT	Computed tomography
C-index	Concordance index
CECT	Contrast-enhanced CT
CAN	Copy number alterations
dCRT	Definite chemoradiotherapy
DWI	Diffusion-weighted imaging
DWI	Diffusion-weighted imaging
EC	Esophageal cancer
ESCC	Esophageal squamous cell carcinoma
GLCM	Gray-level co-occurrence matrix
GLRLM	Gray-level run-length matrix
GLSZM	Gray-level size zone matrix
GTV	Gross tumor volume
KM	Kaplan-Meier
LASSO	Least absolute shrinkage and selection operator
MR	Magnetic resonance

MRI	Magnetic resonance imaging
NGTDM	Neighborhood gray-tone difference matrix features
OAR	Organ at risk
OS	Overall survival
PGTV	Planning gross tumor volume
PTV	Planning target volume
PET-CT	Positron emission tomography-computed tomography
pre-NLR	Pre-treatment neutrophil to lymphocyte ratio
EQD2	Radiation Equivalent Dose in 2 Gy/f
ROC	Receiver operation characteristics
SIB-RT	Simultaneous integrated boost radiotherapy
T2WI-FS	T2-weighted imaging fat suppression
T2WI	Turbo T2-weighted imaging
VOI	Volume of interest

Supplementary Information

The online version contains supplementary material available at <https://doi.org/10.1186/s12885-025-13996-2>.

Supplementary Material 1
Supplementary Material 2
Supplementary Material 3
Supplementary Material 4

Author contributions

Nuo Yu, data curation, formal analysis, investigation, methodology, software, supervision, validation, visualisation, writing – original draft, and writing – review & editing – review & editing. Yidong Wan, data curation, formal analysis, investigation, methodology, software, supervision, validation, visualisation, writing – original draft. Lijing Zuo, methodology, writing – original draft, and writing – review & editing – review & editing. Ying Cao, methodology, writing – original draft, and writing – review & editing – review & editing. Dong Qu, methodology, software, supervision, validation, visualisation. Wenyang Liu, methodology, software, supervision, validation, visualisation. Lei Deng, methodology, software, supervision, validation, visualisation. Tao Zhang, methodology, software, supervision, validation, visualisation. Wenqing Wang, methodology, software, supervision, validation, visualisation. Jianyang Wang, methodology, software, supervision, validation, visualisation. Jima Lv, methodology, software, supervision, validation, visualisation. Zefen Xiao, methodology, software, supervision, validation, visualisation. Qinfu Feng, methodology, software, supervision, validation, visualisation. Zongmei Zhou, methodology, software, supervision, validation, visualisation. Nan Bi, methodology, software, supervision, validation, visualisation. Tianye Niu, conceptualisation, formal analysis, investigation, methodology, project administration, resources, software, supervision, validation, visualisation, and writing – review & editing. Xin Wang, conceptualisation, formal analysis, investigation, methodology, project administration, resources, software, supervision, validation, visualisation, and writing – review & editing.

Funding

Beijing Xisike Clinical Oncology Research Foundation. Item number: Y-Young2023-0114.

Data availability

Research data are stored in an institutional repository and will be shared upon request to the corresponding author.

Declarations

Ethics approval and consent to participate

The study protocol was approved by the ethics committee of Cancer Hospital, Chinese Academy of Medical Sciences and Peking Union Medical College and is registered at clinicaltrials.gov ("NCT02988921"). All patients provided written informed consent.

Consent for publication

Not applicable.

Disclosure

The abstract of this manuscript has been published on the International Journal of Radiation Oncology, Biology, Physics due to the ASTRO meeting.

Competing interests

The authors declare no competing interests.

Author details

¹Department of Radiotherapy, National Cancer Center/National Clinical Research Center for Cancer/Cancer Hospital, Chinese Academy of Medical Sciences and Peking Union Medical College, Beijing, China

²Institute of Translational Medicine, Zhejiang University, Hangzhou, Zhejiang, China

³Department of Radiology, National Cancer Center/National Clinical Research Center for Cancer/Cancer Hospital, Chinese Academy of Medical Sciences and Peking Union Medical College, Beijing, China

⁴Institute of Biomedical Engineering, Shenzhen Bay Laboratory, Gaoke International Innovation Center, Guangqiao Road, Guangming District, Shenzhen, China

Received: 28 April 2024 / Accepted: 24 March 2025

Published online: 02 April 2025

References

- Sung H, Ferlay J, Siegel RL, et al. Global cancer statistics 2020: GLOBOCAN estimates of incidence and mortality worldwide for 36 cancers in 185 countries. *CA Cancer J Clin*. 2021;71:209–49.
- Wang X, Liang F, Wang X et al. Quality of life and survival outcomes of patients with inoperable esophageal squamous cell carcinoma after definitive radiation therapy: A multicenter retrospective observational study in China from 2015 to 2016. *J Natl Cancer Cent*. 2023;3(2):150–158.
- Lambin P, Rios-Velazquez E, Leijenaar R, et al. Radiomics: extracting more information from medical images using advanced feature analysis. *Eur J Cancer*. 2012;48:441–6.
- Gillies RJ, Kinahan PE, Hricak H. Radiomics: images are more than pictures, they are data. *Radiology*. 2016;278:563–77.
- Shi Z, Zhang Z, Liu Z, et al. Methodological quality of machine learning-based quantitative imaging analysis studies in esophageal cancer: a systematic review of clinical outcome prediction after concurrent chemoradiotherapy. *Eur J Nucl Med Mol Imaging*. 2022;49:2462–81.
- Wang L, Gao Z, Li C, et al. Computed Tomography-Based Delta-Radiomics analysis for discriminating radiation pneumonitis in patients with esophageal cancer after radiation therapy. *Int J Radiat Oncol Biol Phys*. 2021;111:443–55.
- Lu N, Zhang WJ, Dong L, et al. Dual-region radiomics signature: integrating primary tumor and lymph node computed tomography features improves survival prediction in esophageal squamous cell cancer. *Comput Methods Programs Biomed*. 2021;208:106287.
- Jin X, Zheng X, Chen D, et al. Prediction of response after chemoradiation for esophageal cancer using a combination of dosimetry and CT radiomics. *Eur Radiol*. 2019;29:6080–8.
- Yang M, Hu P, Li M, et al. Computed Tomography-Based radiomics in predicting T stage and length of esophageal squamous cell carcinoma. *Front Oncol*. 2021;11:722961.
- Lee SL, Yadav P, Starekova J, et al. Diagnostic performance of MRI for esophageal carcinoma: A systematic review and Meta-Analysis. *Radiology*. 2021;299:583–94.
- Leefflang M. The accuracy of MRI for esophageal cancer staging. *Radiology*. 2021;299:595–6.
- Borggreve AS, Goense L, van Rossum P, et al. Preoperative prediction of pathologic response to neoadjuvant chemoradiotherapy in patients with esophageal cancer using (18)F-FDG PET/CT and DW-MRI: A prospective multicenter study. *Int J Radiat Oncol Biol Phys*. 2020;106:998–1009.
- Hirata A, Hayano K, Ohira G, et al. Volumetric histogram analysis of apparent diffusion coefficient as a biomarker to predict survival of esophageal cancer patients. *Ann Surg Oncol*. 2020;27:3083–9.
- Hirata A, Hayano K, Ohira G, et al. Volumetric histogram analysis of apparent diffusion coefficient for predicting pathological complete response and survival in esophageal cancer patients treated with chemoradiotherapy. *Am J Surg*. 2020;219:1024–9.

15. Li ZY, Wang XD, Li M, et al. Multi-modal radiomics model to predict treatment response to neoadjuvant chemotherapy for locally advanced rectal cancer. *World J Gastroenterol*. 2020;26:2388–402.
16. Li C, Ni W, Wang X, et al. A phase I/II radiation dose escalation trial using simultaneous integrated boost technique with elective nodal irradiation and concurrent chemotherapy for unresectable esophageal cancer. *Radiat Oncol*. 2019;14:48.
17. Li C, Wang X, Wang X, et al. A multicenter phase III study comparing simultaneous integrated boost (SIB) radiotherapy concurrent and consolidated with S-1 versus SIB alone in elderly patients with esophageal and esophagogastric cancer - the 3JECROG P-01 study protocol. *BMC Cancer*. 2019;19:397.
18. Pasini G, Stefano A, Russo G, Comelli A, Marinozzi F, Bini F. Phenotyping the histopathological subtypes of Non-Small-Cell lung carcinoma: how beneficial is radiomics. *Diagnostics (Basel)*. 2023;13:1167. <https://doi.org/10.3390/diagnostics13061167>.
19. Huynh E, Coroller TP, Narayan V, Agrawal V, Hou Y, Romano J, et al. CT-based radiomic analysis of stereotactic body radiation therapy patients with lung cancer. *Radiother Oncol*. 2016;120:258–66. <https://doi.org/10.1016/j.radonc.2016.05.024>.
20. Vallières M, Freeman CR, Skamene SR, El Naqa I. A radiomics model from joint FDG-PET and MRI texture features for the prediction of lung metastases in soft-tissue sarcomas of the extremities. *Phys Med Biol*. 2015;60:5471–96.
21. Huang Y, Liu Z, He L, et al. Radiomics signature: A potential biomarker for the prediction of Disease-Free survival in Early-Stage (I or II) Non-Small cell lung cancer. *Radiology*. 2016;281:947–57.
22. Xie C, Yang P, Zhang X, et al. Sub-region based radiomics analysis for survival prediction in oesophageal tumours treated by definitive concurrent chemoradiotherapy. *EBioMedicine*. 2019;44:289–97.
23. Hu T, Wang S, Huang L, et al. A clinical-radiomics nomogram for the pre-operative prediction of lung metastasis in colorectal cancer patients with indeterminate pulmonary nodules. *Eur Radiol*. 2019;29:439–49.
24. Foley KG, Shi Z, Whybra P, et al. External validation of a prognostic model incorporating quantitative PET image features in oesophageal cancer. *Radiother Oncol*. 2019;133:205–12.
25. Xiong J, Yu W, Ma J, Ren Y, Fu X, Zhao J. The role of PET-Based radiomic features in predicting local control of esophageal cancer treated with concurrent chemoradiotherapy. *Sci Rep*. 2018;8:9902.
26. Tang S, Ou J, Liu J, et al. Application of contrast-enhanced CT radiomics in prediction of early recurrence of locally advanced oesophageal squamous cell carcinoma after trimodal therapy. *Cancer Imaging*. 2021;21:38.
27. Larue R, Klaassen R, Jochems A, et al. Pre-treatment CT radiomics to predict 3-year overall survival following chemoradiotherapy of esophageal cancer. *Acta Oncol*. 2018;57:1475–81.
28. Xie SH, Zhang WF, Wu Y, Tang ZL, Yang LT, Xue YJ, et al. Application of predictive model based on CT radiomics and machine learning in diagnosis for occult locally advanced esophageal squamous cell carcinoma before treatment: A two-center study. *Transl Oncol*. 2024;47:102050. <https://doi.org/10.1016/j.tranon.2024.102050>.
29. Gong J, Zhang W, Huang W, et al. CT-based radiomics nomogram May predict local recurrence-free survival in esophageal cancer patients receiving definitive chemoradiation or radiotherapy: A multicenter study. *Radiother Oncol*. 2022;174:8–15.
30. Chu F, Liu Y, Liu Q, et al. Development and validation of MRI-based radiomics signatures models for prediction of disease-free survival and overall survival in patients with esophageal squamous cell carcinoma. *Eur Radiol*. 2022;32:5930–42.
31. Kawada S, Imai Y. [Diagnosis of esophageal cancer and metastatic lymph node using CT and MRI]. *Nihon Rinsho*. 2011;69(Suppl 6):174–81.
32. Qu J, Zhang H, Wang Z, et al. Comparison between free-breathing radial VIBE on 3-T MRI and endoscopic ultrasound for preoperative T staging of resectable oesophageal cancer, with histopathological correlation. *Eur Radiol*. 2018;28:780–7.
33. De Cecco CN, Ciolina M, Caruso D, et al. Performance of diffusion-weighted imaging, perfusion imaging, and texture analysis in predicting tumoral response to neoadjuvant chemoradiotherapy in rectal cancer patients studied with 3T MR: initial experience. *Abdom Radiol (NY)*. 2016;41:1728–35.
34. Hardiman KM, Antunez AG, Kanters A, Schuman AD, Regenbogen SE. Clinical and pathological outcomes of induction chemotherapy before neoadjuvant radiotherapy in locally-advanced rectal cancer. *J Surg Oncol*. 2019;120:308–15.
35. Larue R, Van De Voorde L, van Timmeren JE, et al. 4DCT imaging to assess radiomics feature stability: an investigation for thoracic cancers. *Radiother Oncol*. 2017;125:147–53.
36. Petralia G, Padhani AR, Pricolo P, et al. Whole-body magnetic resonance imaging (WB-MRI) in oncology: recommendations and key uses. *Radiol Med*. 2019;124:218–33.
37. Lu S, Wang C, Liu Y et al. The MRI radiomics signature can predict the pathologic response to neoadjuvant chemotherapy in locally advanced esophageal squamous cell carcinoma. *Eur Radiol*. 2024;34(1):485–494.
38. Giger A, Stadelmann M, Preiswerk F, et al. Ultrasound-driven 4D MRI. *Phys Med Biol*. 2018;63:145015.
39. Lau D, Chen Z, Teo JT, et al. Intensity-modulated microbend fiber optic sensor for respiratory monitoring and gating during MRI. *IEEE Trans Biomed Eng*. 2013;60:2655–62.
40. Beukinga RJ, Wang D, Karrenbeld A, et al. Addition of HER2 and CD44 to (18)F-FDG PET-based clinico-radiomic models enhances prediction of neoadjuvant chemoradiotherapy response in esophageal cancer. *Eur Radiol*. 2021;31:3306–14.
41. Yu KH, Zhang C, Berry GJ, et al. Predicting non-small cell lung cancer prognosis by fully automated microscopic pathology image features. *Nat Commun*. 2016;7:12474.
42. Feng L, Liu Z, Li C, et al. Development and validation of a radiopathomics model to predict pathological complete response to neoadjuvant chemoradiotherapy in locally advanced rectal cancer: a multicentre observational study. *Lancet Digit Health*. 2022;4:e8–17.
43. Qi WX, Li S, Xiao J, Li H, Chen J, Zhao S. A machine learning approach using (18)F-FDG PET and enhanced CT scan-based radiomics combined with clinical model to predict pathological complete response in ESCC patients after neoadjuvant chemoradiotherapy and anti-PD-1 inhibitors. *Front Immunol*. 2024;15:1351750. <https://doi.org/10.3389/fimmu.2024.1351750>.
44. Simoni N, Rossi G, Benetti G, Zuffante M, Micera R, Pavarana M, et al. (18) F-FDG PET/CT metrics are correlated to the pathological response in esophageal cancer patients treated with induction chemotherapy followed by neoadjuvant Chemo-Radiotherapy. *Front Oncol*. 2020;10:599907. <https://doi.org/10.3389/fonc.2020.599907>.
45. Deantonio L, Garo ML, Paone G, Valli MC, Cappio S, La Regina D, et al. 18F-FDG PET radiomics as predictor of treatment response in oesophageal cancer: A systematic review and Meta-Analysis. *Front Oncol*. 2022;12:861638. <https://doi.org/10.3389/fonc.2022.861638>.
46. Bi WL, Hosny A, Schabath MB, Giger ML, Birkbak NJ, Mehrtash A, et al. Artificial intelligence in cancer imaging: clinical challenges and applications. *CA Cancer J Clin*. 2019;69:127–57. <https://doi.org/10.3322/caac.21552>.
47. Luca Cairone VB, Samuel Bignardi FM, Anthony Yezzi AT, Giuseppe Salvaggio FB&AC. Robustness of radiomics features to varying segmentation algorithms in magnetic resonance images. *Image Anal Process*. 2022. https://doi.org/10.1007/978-3-031-13321-3_41. Lecture Notes in Computer Science.

Publisher's note

Springer Nature remains neutral with regard to jurisdictional claims in published maps and institutional affiliations.